Proceedings of the 11th Polish–Japanese Joint Seminar on Micro and Nano Analysis, Gniew, September 11–14, 2016

Metrology and 3D Imaging of Microstructural Elements in Materials for Environmentally Friendly Power Plants

A. Kruk* and A. Czyrska-Filemonowicz

AGH University of Science and Technology, International Centre of Electron Microscopy for Materials Science & Faculty of Metals Engineering and Industrial Computer Science, Al. A. Mickiewicza 30, 30-059 Krakow, Poland

The aim of this study was the application of tomographic techniques (focused ion beam–scanning electron microscopy, scanning transmission electron microscopy–energy-dispersive X-ray spectroscopy) to qualitative and quantitative characterization of structural elements in T/P92 creep resistant 9% Cr steel, Allvac 718Plus Ni-based superalloy and W-based alloy — multiphase materials for environmentally friendly power plants exposed to extreme operational conditions. The study showed that tomography techniques permit to obtain complementary information about microstructural features (precipitates size, shape and their spatial distribution) in the reconstructed volume with comparison to conventional particle analysis methods, e.g. quantitative transmission electron microscopy and scanning electron microscopy metallography.

DOI: 10.12693/APhysPolA.131.1311

PACS/topics: 06.90.+v, 87.64.Ee, 81.05.Bx

1. Introduction

The development of materials for extreme conditions and environmentally friendly energy systems requires an application of innovative materials and use of 3D image techniques for characterization their structure down to nanoscale or even atomic scale. Application of tomography techniques, such as transmission electron microscopy/scanning transmission electron microscopy (TEM/STEM) electron tomography and focused ion beam–scanning electron microscopy (FIB–SEM) tomography, provides new opportunities. Those techniques allow reconstructing the microstructure of investigated materials in three dimensions. The TEM/STEM electron and FIB–SEM tomography techniques have been adopted with a big success by researchers to materials science [1, 2]. The resolution (determined as a voxel size) in 3D reconstructions, however, depends on applied tomographic technique and varies from tenths parts to few tens of nm. The tomography in material sciences is currently a relatively new technique that uses a TEM or dual beam workstation FIB–SEM to 3D imaging of microstructural elements in any engineering materials. The TEM electron tomography using high angle annular dark field (HAADF), energy-dispersive X-ray spectroscopy (EDX) or energy filtered transmission electron microscopy (EFTEM) imaging methods was developed to reconstruct objects in three dimensions (3D) from a tilt series of 2D images [3]. The TEM electron tomography technique enables obtaining 3D model of the investigated object(s) from the multiple 2D projection images, acquired over a range of viewing directions (±75°). This technique was earlier used and was well accepted in the life sciences as a method used to study viruses or cells as well as for visualization and metrology of structural elements in metallic alloys.

FIB–SEM tomography is based on a serial slicing technique using a FIB–SEM dual beam workstation described in detail in Ref. [4]. Precise *in-situ*milling was performed by Ga+ ion beam with about few nm thick steps. For dual-beam SEM enables the acquisition of serial images with small (few nm) and reproducible spacing between the single imaging planes. With the help of computer software for digital processing of data stacks and graphics packages for visualization 3D volume can be easily reconstructed and the structure interrogated to obtain both: qualitative and quantitative information. It is possible to study features at spatial resolutions at the tens-of-nm level and volumes with dimensions of up to tens of micrometers.

2. Experimental details and results

2.1. FIB–SEM tomography

In order to achieve higher efficiency and reduce CO_2 emission and other environmentally damaging gases, new power generation technology requires high pressure and high temperature parameters of steam. These have directly resulted in the introduction of ultra-super critical (USC) plants and application of creep resistant 9–12%Cr steels. Among them, the T/P92 martensitic steel, which has creep strength 25–30% higher than the widely used modified 9%Cr steel T/P91. The important microstructural changes during creep deformation at elevated temperatures of P92 steel were size, morphology and distribution of the $M_{23}C_6$ and MX (X = C and/or N) precipitates as well as the chemical composition of the precipitates and the matrix. In the steel exposed for longer time, the Laves phase Fe_2(W,Mo) and other intermetallic phases were formed [5].

*corresponding author; e-mail: kruczek@agh.edu.pl

The FIB NEON CrossBeam 40EsB with Ga-ion beam at parameters: 30 kV, 200 pA and aperture of 30 μm was used to perform a precise *in situ* milling. Repeated removal of layers as thin as a 15 nm allowed exploring a total volume of $14 \times 66 \times 56$ μm^3 ($V = 5174$ μm^3). Consequently, the acquired stack of images (image size 1024×768 pixels, 378 images in 8-bit grayscale, stack size 147 MB) was transformed directly into a 3D data volume with a voxel size of $15 \times 15 \times 15$ nm^3. The shift of the electron beam in lateral direction due to slice cutting during recording of the tomogram was calculated and subsequently corrected with the ImageJA 1.45b software. From the series of SEM micrographs, the 3D reconstruction of the investigated alloy volume was generated by ImageJ 1.45b and Avizo Fire 6.3 software. Visualization of microstructural elements using FIB–SEM slicing techniques were presented in Fig. 1 showing the spatial distribution of precipitates such as Laves phase, $M_{23}C_6$ carbides and MX carbonitrides existing in tomographic reconstructed volume. Figure 1a shows an enlarged fragment of reconstructed volume which shows the morphology (complex shape) of the selected precipitates of the Laves phase particles. The largest dimension of the particles exceeds 1 μm. Carbide and carbonitrides precipitates are much smaller than the Laves phase particles and are uniformly distributed over the whole volume.

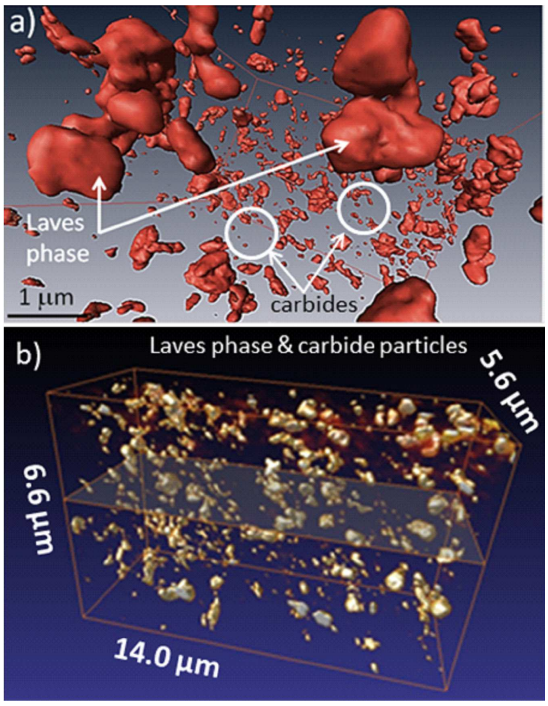

Fig. 1. Results of FIB–SEM tomography application for 3D visualization of microstructural elements in P92 steel: (a) morphology of selected Laves phase, carbide and carbonitride particles observed in the enlarged fragment of reconstructed volume, (b) spatial distribution of precipitates (Laves phase, $M_{23}C_6$ carbides and MX carbonitrides) existing in tomographic reconstructed volume of $14 \times 6.6 \times 5.6$ μm^3.

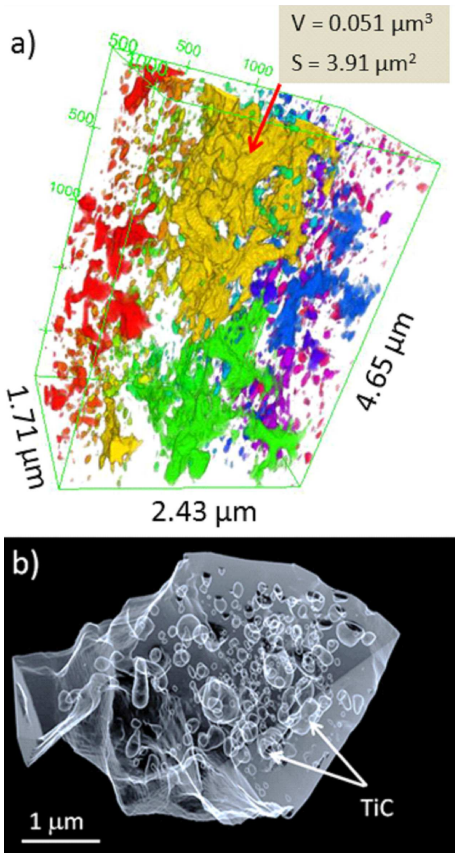

Fig. 2. Three-dimensional visualization of spatial shape of porous and carbide particles in W–1.7%TiC alloy: (a) 3D visualization of reconstructed volume ($2.43 \times 1.71 \times 4.65$ μm), varied in respect of the pore dimensions are labeled with a different color. The largest pore marked in yellow, a smaller green and the other is red and blue. Voxel size is $3.8 \times 3.8 \times 5$ nm. (b) Result of tomographic reconstruction (3D visualization) of a single grain with visible carbide particles inside grain.

The next example of materials examined utilizing FIB–SEM tomography is the W–1.7%TiC alloy. Tungsten and its alloys are considered as potential candidates for plasma facing materials, particularly in the divertor and the first wall in nuclear fusion reactor due to the low sputtering rate, high thermal conductivity, high strength at elevated temperatures and low tritium inventory. The divertor design requires a material having a low ductile–brittle transition temperature (DBTT) and recrystallization temperature (TR) around 1300 °C. One new material under consideration is W–1.7%TiC alloy [6, 7]. Addition of carbides stabilizes the tungsten microstructure at elevated temperatures and contributes to improve the strength of tungsten and as well as DBTT and TR. 3D visualization of pores in tungsten-base alloy is presented in Fig. 2. The reconstructed volume was $4.21 \times 3.7 \times 0.3$ μm^3. The pores can be divided into large irregular shaped (volume highlighted in yellow in Fig. 1a; volume $V = 0.051$ μm^3, surface $S = 3.91$ μm^2) and small oval in shape, marked in different colours. Figure 2b shows the result of tomographic reconstruction

(3D visualization) of a single grain with visible carbide precipitates inside grains. Quantitative analysis, performed on the tomographic reconstructed volume, has enabled to determine the basic stereological parameters (volume fraction V_v, mean diameter D) of the microstructural elements. The results of the analysis were the following: V_v(carbides) $= 0.57 \pm 0.09\%$ with mean diameter $D = 13.4$ nm, V_v(pores) $= 4.41 \pm 0.62\%$ and $D = 48.6$ nm. Mean diameter of particles in that volume was estimated as 32.6 ± 18.8 nm.

Another structural material, where FIB–SEM imaging techniques (with FIB parameters: 30 kV, $I = 1$ nA, voxel size $18 \times 18 \times 36$ nm^3, SEM imaging with EsB detector at 2 kV) was applied for the visualization of microstructural elements, is as-cast Allvac 718Plus superalloy [8–11]. This is a newly developed Ni-based superalloy for application in power generation and aeronautics, which exhibits high strength and oxidation resistance as well as improved high temperature performance compared to the Inconel 718 superalloy. The as-cast 718Plus superalloy subjected heat treatment 1200 °C/4 h + 986 °C/10 h and ageing at 788 °C/8 h and 704 °C/8 h has the microstructure which consists of a γ dendrite matrix with two kinds of eutectics (MC-type carbides $+\gamma$-phase) and (Laves-phase $+\gamma$-phase) precipitates in inter-dendritic region, Fig. 3a. This heat treatment leads to the precipitation of γ'-Ni_3(Al,Ti) in all alloy volume and platelet precipitates of η-Ni_3Ti phases nucleating at Laves phase, Fig. 3a,b. Figure 3b shows the result of tomographic reconstruction (3D visualization) of a Laves phase with η-phase plates particles which precipitation starts at the surface of the Laves phase.

It should be noted that the result of 3D imaging is influenced by many material and experimental factors. One of the important steps for FIB–SEM tomography investigation is selection of an interesting area — region of interest (ROI). Choice of the place depends on the contrast between different microstructural features during SEM–backscattered electrons (SEM–BSE) observation. The observed contrast depends on the difference of the chemical composition (Z-contrast) between the microstructural elements. Another factor influencing on the differences in contrast between grains with different crystallographic orientation is result of the occurrence of the channeling effect. The result of electron channeling is the combination of imaging and orientation information which is available in the SEM during imaging at low acceleration voltages (few kV) using BSE detector.

2.2. STEM electron tomography

The electron tomography study of Allvac 718Plus (718Plus) superalloy was conducted on the lamella prepared by FIB (NEON CrossBeam 40EsB) using a probe Cs corrected Titan^3 G2 60-300 with ChemiSTEM™ system with Super-X detector. This EDX detection system allowed to achieve a high level of X-ray signal over a large tilt angle of sample and collect series of 2D elemental maps in the angular range from $-60°$ to $+60°$ with step of 4°. Pre-processing and alignment of image tilt series

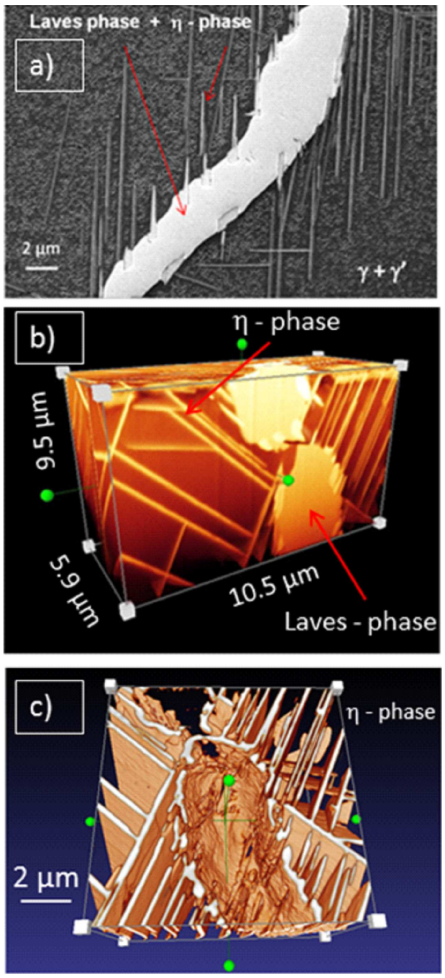

Fig. 3. Result of tomographic reconstruction (3D visualization) of a Laves phase with η-phase plates particles: (a) Laves phase with η-phase plate particles which precipitation starts at the interface of the Laves phase, SEM–BSE, (b) 3D visualization of tomographic reconstructed volume $10.5 \times 9.5 \times 5.9$ μm, (c) visualization of a Laves phase with η-phase rendered from reconstructed volume.

were performed using TomoJ 2.12 software. Tomographic reconstruction of a tilt series of 31 images (chemical element maps) was performed using simultaneous iterative reconstructive technique (SIRT) method [12] with number of iteration equal to 12, which allowed visualizing the three-dimensional distribution of selected elements (Al, Cr) in the analysed volume. STEM–EDX elemental Al map selected from the registered tilt series is presented in Fig. 4a. The results of 3D visualization of the shape and distribution of γ' particles in 718Plus superalloy using STEM–EDX tomography technique are shown in Fig. 4b. It can be observed that γ' phase particles are spherical. The volume fraction (V_v) of γ' phase and the mean equivalent particle diameter (D_{eq}) in the reconstructed volume were as follows: $V_v = 12.5\%$ and $D_{eq} = 26.0 \pm 8.3$ nm.

Qualitative and quantitative evaluation of the strengthening particles of γ' phase in 718Plus superal-

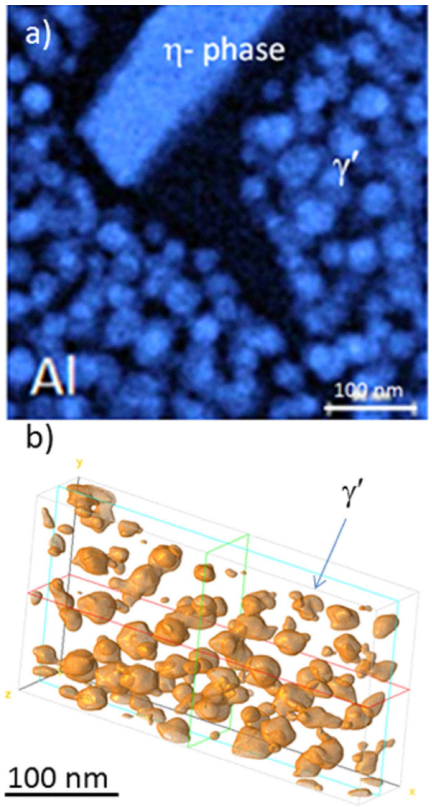

Fig. 4. Visualization of γ' particles in 718Plus superalloy. Volume reconstruction was performed using electron (STEM–EDX) tomography technique: (a) STEM–EDX elemental map of Al, (b) 3D visualization of tomographic reconstructed γ' particles.

loy by STEM–EDX tomography was conducted with the resolution about of 0.2 nm.

The reconstruction imperfections are mainly the result of the limited tilt range on the TEM. Resolution in a tomographic reconstruction is anisotropic. Parallel to the tilt axis, the resolution is defined by the resolution in the images acquired. Perpendicular to tilt axis resolution depends on sample thickness, number of images and missing wedge — tilt range.

3. Summary

TEM/STEM electron tomography and FIB–SEM tomography techniques are promising tools in material science for quantitative characterization of the internal structure components and/or the spatial distribution and particles morphology in a solid material. Those methods are complementary to conventional particle analysis methods, e.g. quantitative TEM/SEM metallography. However, the results of 3D imaging are influenced by many material and experimental factors. The FIB–SEM tomography results of different structural materials confirmed the ability of this technique to obtain 3D reconstruction of the objects of 100 nm or even smaller, however selecting the SEM imaging method (SEM–SE, SEM–BSE) has significant influence on the results of qualitative and quantitative assessment of microstructural elements.

Tomographic reconstruction performed using STEM–EDX technique allowed for 3D visualization of the precipitates shapes, spatial distribution and perform qualitative and quantitative evaluation of γ' precipitates in the 718Plus superalloy. Due to new possibilities offered by a ChemiSTEM™ system (with a Super-X detector), high level of X-ray signal over a large tilt angle (±60°) of sample was achieved and series of 2D elemental maps were collected. X-ray spectroscopic imaging (STEM–EDX), enables the mapping of local concentrations of selected chemical elements. This technique was used for qualitative and quantitative evaluation of the strengthening coherent particles of γ' phase in 718Plus superalloy.

Acknowledgments

The authors acknowledge the support from Polish Ministry of Science and Higher Education project no. 2832/7PR/2013/2 (SPB-ESTEEM2 AGH project no. 22.22.110.70029). The authors thank Mr. A. Gruszczyński, M.Sc. (AGH-UST), for his assistance in the FIB–SEM investigations.

References

[1] K. Kulawik, P.A. Buffat, A. Kruk, A. Wusatowska-Sarnek, A. Czyrska-Filemonowicz, *Mater. Character.* **100**, 74 (2015).

[2] A. Kruk, A. Czyrska-Filemonowicz, *Arch. Metall. Mater.* **58**, No. 2 (2013).

[3] P.A. Midgley, R.E. Dunin-Borkowski, *Nature Mater.* **8**, 271 (2009).

[4] A. Kruk, G. Cempura, S. Lech, A. Czyrska-Filemonowicz, *Arch. Metall. Mater* **61**, No. 2 (2016).

[5] A. Czyrska-Filemonowicz, P.J. Ennis, A. Zielińska-Lipiec, *Metallurgy on the Turn of the 20th Century*, Ed. K. Swiątkowski, Polish Academy of Sciences, AKAPIT, Kraków 2002.

[6] N.P. Taylor, C.B.A. Forty, D.A. Petti, K.A. McCarthy, *J. Nucl. Mater.* **283-287**, 28 (2000).

[7] G. Cempura, A. Kruk, C. Thomser, M. Wirtz, A. Czyrska-Filemonowicz, *Arch. Metall. Mater.* **58**, No. 2 (2013).

[8] R.M. Kearsey, J. Tsang, S. Oppenheimer, E. Mcdevitt, *JOM* **64**, 241 (2012).

[9] X. Xie, C. Xu, G. Wang, J. Dong, W.-D. Cao, R. Kennedy, in: *Superalloys 718, 625, 706 and Derivatives 2005*, Ed. E.A. Loria, The Minerals, Metals & Materials Society, Pittsburgh 2005.

[10] W.D. Cao, R.L. Kennedy, in: *Superalloys 2004, Seven Springs Conf., Seven Springs Conf*, Eds. K.A. Green, T.M. Pollock, H. Harada, The Minerals, Metals & Materials Society, Pittsburgh 2004.

[11] E.J. Pickering, H. Mathur, A. Bhowmik, O.M.D.M. Messé, J.S. Barnard, M.C. Hardy, R. Krakow, K. Loehnert, H.J. Stone, C.M.F. Rae, *Acta Mater.* **60** , 2757 (2012).

[12] P.C. Gilbert, *J. Theor. Biol.* **36**, 105 (1972).